

Montel for ID20

Aouadi Yiones

October 30, 2018

1 Introduction

With the following document I want to report the results obtained in the simulation of a beam through a Montel system (optical system composed by two orthogonal mirrors). It has been studied the tolerance in orthogonality using the parameter similar to those distributed by the AXO DRESDEN GmbH [Gmb17]

2 System

In this simulation was used a Monte-Carlo approach with the following specification

2.1 Source

Source parameters

- Number of rays: 10^6
- Source size: $1 \times 1 \mu m^2$
- Divergence: gaussian profile with a FWHM OF $25 \mu rad$ ($\sigma = 10.6 \mu rad$)

Figure 1 show the source geometry and the divergence of the source beam

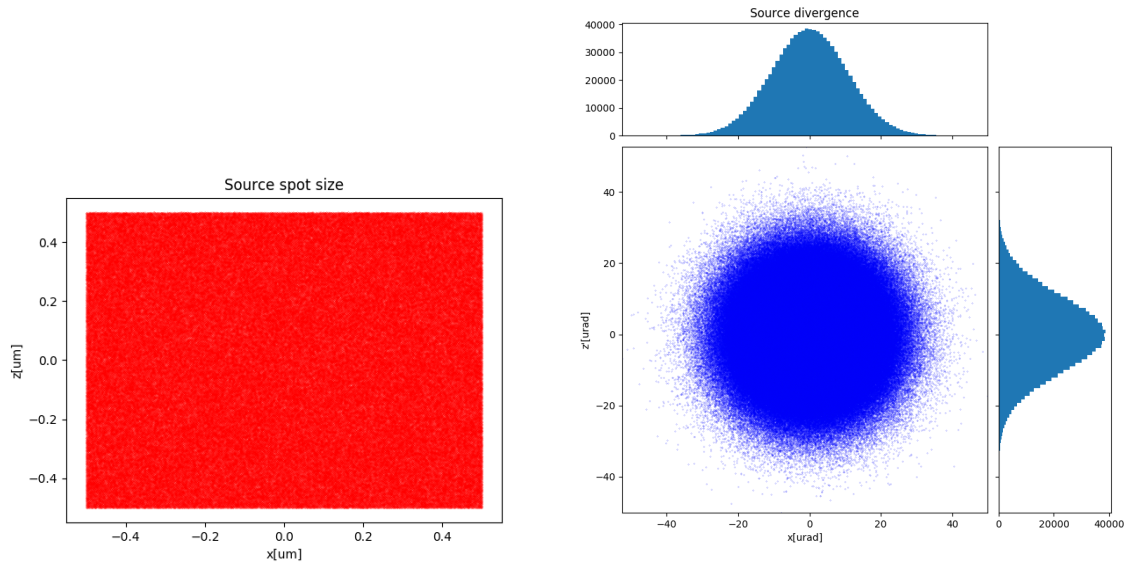


Figure 1: Source size $1 \times 1 \mu m^2$

2.2 Montel system

As mentioned before, two orthogonal mirror (parabolic in this case) were used, with parameters

- Focal distance (distance between the source and the center of the mirror): $f=351 mm$

- Mirror length: $L=300mm$
- Mirror width: $W=100mm$
- Δ (error max. between the orthogonal configuration of the two mirrors, negative correspond to have the mirror closer each other, positive further): $\Delta = \pm 0.03^\circ$
- Parabola parameter: $p=0.23mm$, that correspond to an incidence angle of $18.1mrad$ (see appendix A)

In figure 2 is showed a 3Dgraphic view of the Montel system with the parameter used. The reference system is solidale with the Montel system, having the $(0,0,0)$ point at the center of the Montel system.

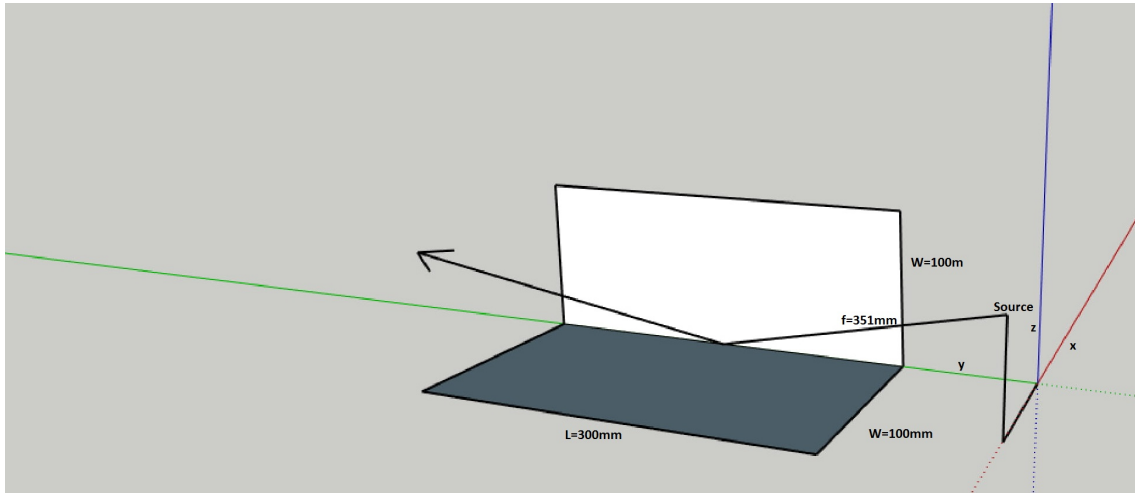


Figure 2: Montel system

3 Results of beam figure and footprint

The image plane is positioned at $1m$ from the center of the Montel system. The property of the beam at the image plane are showed in figure 3. It is obtained a new spot size with a length of $60\mu m$ in the x direction and $100\mu m$ in the z direction, and the divergence has a dimension of $\simeq 40\mu rad$

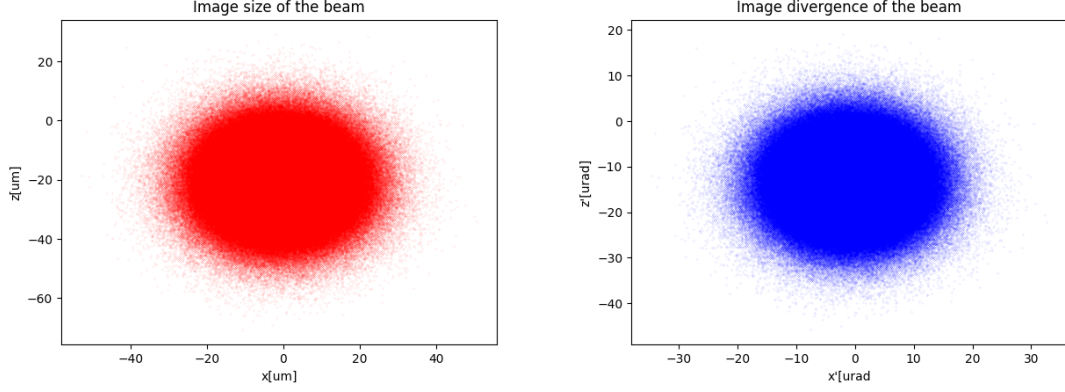


Figure 3: Left image: size of the beam on the image plane. Right image: divergence at the image plane

Moreover is interesting to note the footprint of the two mirror (figure 4) because the area hit by the beam have a greater component on the y direction (due to the grazing incidence), than in the other direction. The x -length of the xy -mirror, and the z -length of the zy -mirror, is very small (at the order of $20\mu m$) with respect to the y -length that is $\simeq 20mm$

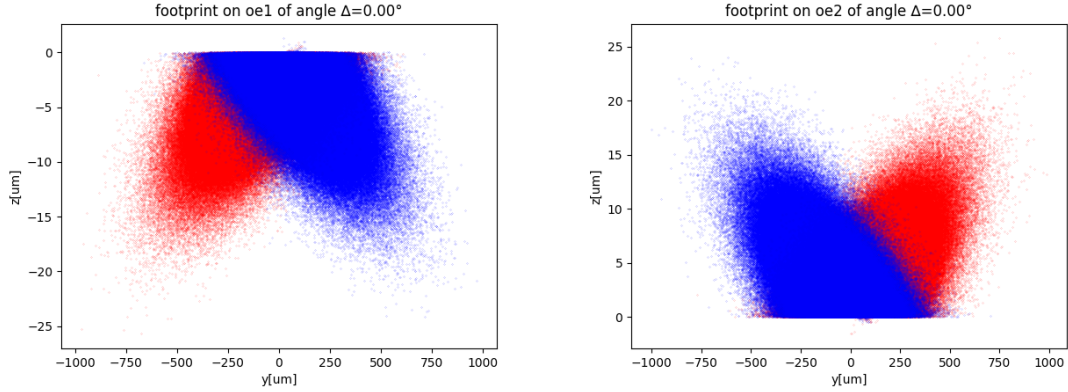


Figure 4: footprint, on the xy -mirror (left figure), zy -mirror (right figure). The red dots are those ray that hit before xy -mirror and after zy -mirror, the blue ones before xy -mirror and after zy -mirror

4 Analysis of orthogonality

Figure 5, 7 presents the interesting histograms versus the horizontal anlage x' when the angle between the mirrors change ($\alpha = 90^\circ + \Delta$). It can be noted a improvement of the collimation of the beam changing the angle in the case of closer mirrors ($\Delta = -0.01^\circ$).

Figure 6 show the trend of the FWHM of the x' changing the angle Δ , it is possible to note a minimum for negative angle (this ideal situation is the pink curve reported in figure 5, 7) after that the situation become worse. Moreover, the behavior of the FWHM is not symmetrical with respect to 0° , in case of negative angle deviation the situation improve for a small range of deviation angle, after that, the trend get worse, on the opposite way, the situation get worse increasing the positive deviation angle.

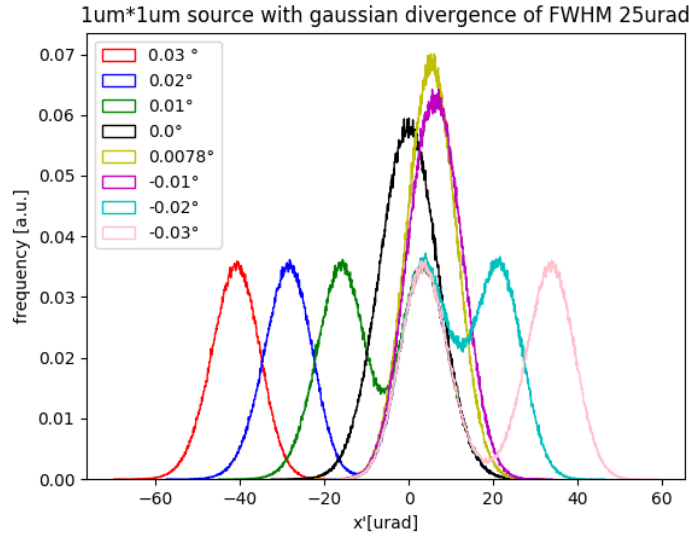


Figure 5: x' values after the Montel system

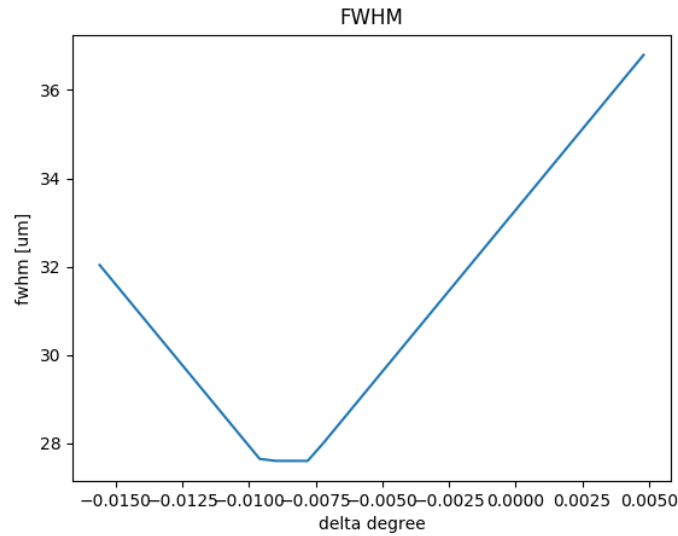


Figure 6: FWHM

1 μ m*1 μ m source with gaussian divergence of FWHM 25 μ rad

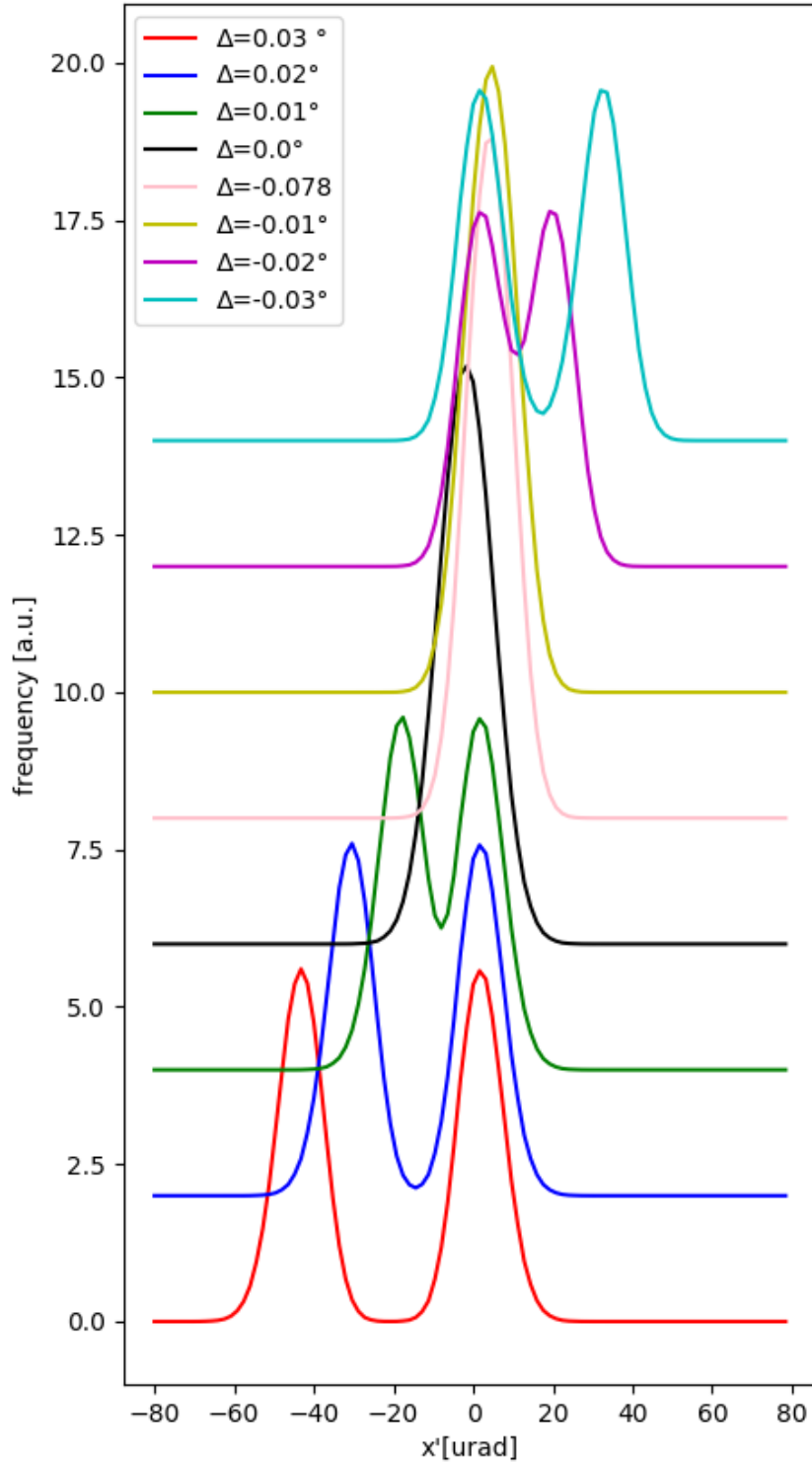


Figure 7: x' values after the Montel system

5 Best Δ

In this section is studied how the different source parameter will influence the best value of delta, The simulation are done playing with the source parameter:

- Source shape: rectangular, circular, gaussian
- Source dimension
- Source divergence

Shape	Dimension	Divergence [μrad]	Minimum α [degree]	Min FWHM [μm]
Gaussian	fwhm of $1\mu\text{m}$	25	-0.008	16.5
Gaussian	fwhm of $1\mu\text{m}$	250	-0.1	165
Gaussian	fwhm of $1\mu\text{m}$	2500	-1	1740
Square	side of $1\mu\text{m}$	25	-0.009	17
Square	side of $1\mu\text{m}$	250	-0.1	161
Square	side of $1\mu\text{m}$	2500	-1	1700
Circular	radius of $\frac{1}{\pi}\mu\text{m}$	25	-0.009	16.4
Circular	radius of $\frac{1}{\pi}\mu\text{m}$	250	-0.1	171
Circular	radius of $\frac{1}{\pi}\mu\text{m}$	2500	-1.35	1760

Table 1: Best Δ value changing the different parameter of the source

Table 1 shows that the source geometry doesn't affects the optimum angle that is ruled by the divergence of the source.

Spot dimension [μm^2]	Divergence [μrad]	Minimum α [degree]	Min FWHM [μm]
1*5	25	-7.6	16.6
2*2.5	25	-7.5	16.8
3*1.67	25	-7.2	16.6
4*1.25	25	-8.8	18
5*1	25	-7.1	17

Table 2: Best Δ value changing the different symmetry of the source

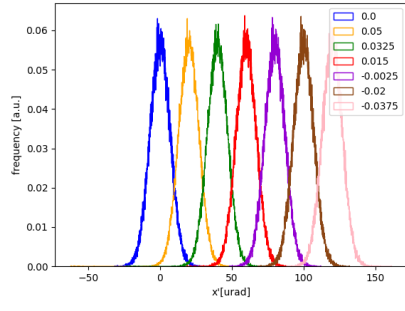
Table 1 shows that the symmetry doesn't affects the optimum angle.

5.1 Best Δ for a non centered beam

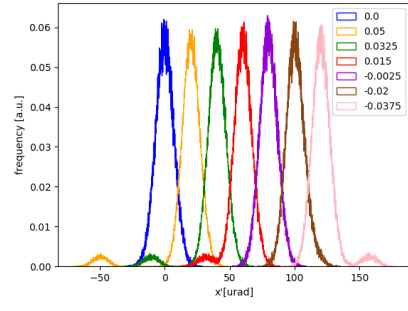
Here is reported the behavior of the beam when it hit a different point of the Montel system. Table 3 is done in this way, the first row and the first coloumn report the point where the beam hit, and, inside the grid, there is the best value of Δ (first row), and the best FWHM(second row).As is showed, the FWHM and the best Δ is less influenced from the y-position than the others Another interesting aspect is that showed in figure , the presence of the second peak decrease with the distance from the $y=0$ axis position

	y=-1mm	y=-0.5mm	y=0	y=0.5	y=1mm
z	-0.015°	-0.015°	-0.015°	-0.015°	-0.018°
20 μm	16.6 μm	16.5 μm	16.5 μm	16.5 μm	18 μm
z	-0.01°	-0.01°	-0.075°	-0.005°	-0.01°
10 μm	16 μm	16 μm	16 μm	16 μm	16 μm
	-0.005°	-0.005°	-0.005°	-0.005°	-0.015°
	14.5 μm	14.5 μm	14.5 μm	14.5 μm	16.6 μm
x	-0.01°	-0.01°	-0.0075°	-0.01°	-0.006°
-10 μm	16 μm	16 μm	16 μm	16 μm	6 μm
x	-0.01°	-0.01°	-0.01°	-0.01°	-0.01°
-20 μm	16.5 μm	16.5 μm	16.5 μm	16.5 μm	16.5 μm

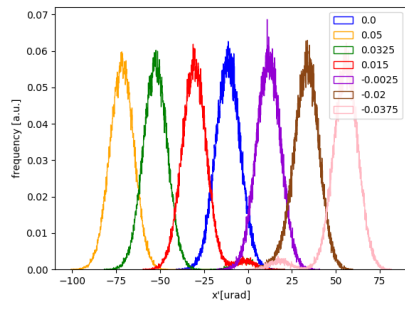
Table 3: Best FWHM and Δ for a non centered beam



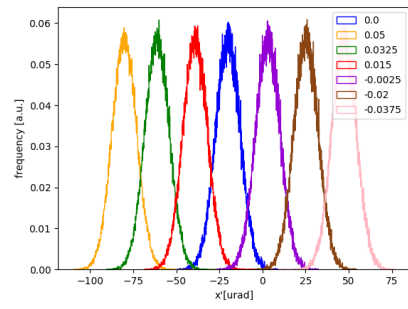
(a) $(-20\mu\text{m}, 0, 0)$



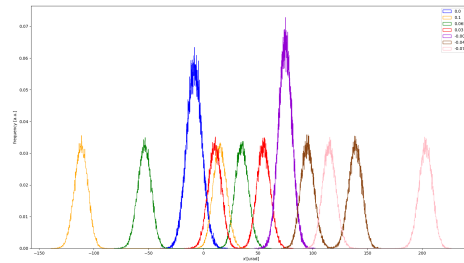
(b) $(-10\mu\text{m}, 0, 0)$



(c) $(0, 0, 10\mu\text{m})$



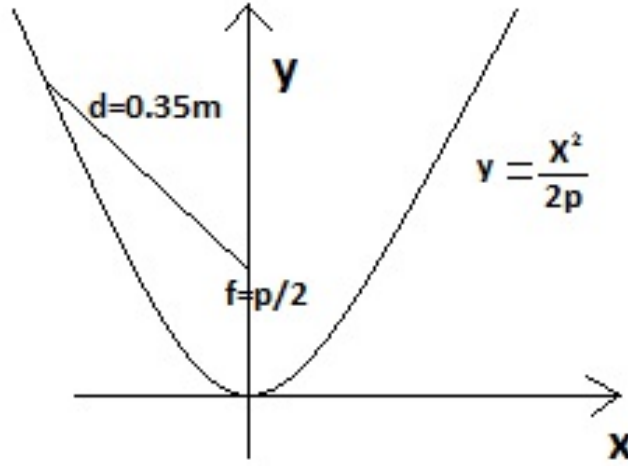
(d) $(0, 0, 20\mu\text{m})$



(e) $(0, 0, 0)$

Figure 8: Beam at the different hitting point (the beam were split on the x-axis)

Appendix A: how to find θ



$$y = \frac{x^2}{2p}$$

$$d = \sqrt{(x_p - x_0)^2 + (y_p - y_0)^2} = \sqrt{x_p^2 + (y_p - \frac{p}{2})^2}$$

$$x_p = -0.0127046, y_p = 0.350885$$

velocity to hit that point starting from $(0, \frac{p}{2})$

$$v_x = -0.0363024, v_y = 0.999341$$

normal at that point

$$n_x = -0.984005, n_y = -0.17814$$

doing dot product between the normal and the velocity is possible to find

$$\theta = \arccos(v_x * n_x + v_y * n_y) = 88.962^\circ$$

[Bau98]

References

[Bau98] Marc Baudoin. *Impara L^AT_EX (e mettilo da parte)*, 1998.

[Gmb17] AXO DRESDEN GmbH. Appendix c-astix for 11.215 kev, feasibility study. 5/05/2017.